Infrared Spectrum of NeHF

David C. Clary, [a] Christopher M. Lovejoy, S. V. ONeil, and David J. Nesbitt [b]

*Joint Institute for Laboratory Astrophysics, National Bureau of Standards and University of Colorado,
Boulder, Colorado 80309-0440*

The infrared-absorption spectrum of the previously unobserved NeHF molecule has been predicted from an *ab initio* quantum-mechanical calculation and subsequently determined for the first time by direct measurement. The two procedures yield remarkable agreement in the positions, widths, and intensities of the infrared spectral lines. The calculations predict, and the experiments confirm, highly unusual vibrational dynamics.

PACS numbers: 33.20.Ea, 33.10.Gx

van der Waals molecular complexes, bound only by long-range electrical-induction effects and the London dispersion energy, and executing extremely wide amplitude vibrational motion, are prototypes for weakly interacting systems ranging from liquids to macromolecules. The vibrational spectra of a number of rare gases—hydrogen halide van der Waals molecules (ArHF,[1,2] KrHF,[2] XeHF,[2] NeHCl,[3] and ArHCl[4-7]) have been characterized recently, but to date one of the simplest rare gases—hydrogen halide complexes, NeHF, has gone unobserved. Simultaneously, computational methods have evolved to the point that reliable characterization of yet unobserved species ought to be possible even for such weakly bonded systems. In this Letter we present the infrared-absorption spectrum of the NeHF molecule, as predicted from an *ab initio* quantum-mechanical calculation[8] and as subsequently determined for the first time by direct measurement. The two procedures yield remarkable agreement in the positions, widths, and intensities of the infrared spectral lines. We also predict and observe novel rotational predissociation dynamics by which one vibrational state is energetically free to dissociate but remains bound by restrictions arising purely from symmetry, and another vibrational state dissociates with a dramatically J-dependent rate.

The infrared NeHF spectrum reported here arises from strong rovibrational transitions of diatomic HF in the presence of a weakly bound Ne atom. The intermolecular potential is sufficiently isotropic that HF behaves as a nearly free rotor, while the HF vibration is essentially decoupled because it is the lone high-frequency mode. Thus, although the only rigorous quantum numbers in this floppy system are total angular momentum (J) and parity, quantum numbers corresponding to the HF rotor angular momentum (j) and its projection (m_j) onto the intermolecular axis are approximately good, as is the orbital angular momentum (l) of neon and HF about their common center of mass. In this language, the Σ, Π^-, and Π^+ upper rovibrational states correlate with the triply degenerate $j=1$ state of free HF, but are split slightly by j-l coupling in the com-

plex. Figure 1 depicts the situation graphically.

The *ab initio* calculations, fully described elsewhere,[10] began with the determination of the NeHF potential-energy surface with coupled-electron-pair approximation[11] correlated wave functions. The contracted Gaussian basis consisted of a $[6s,4p,1d]$ kernel on fluorine and neon, and a $[4s,1p]$ kernel on hydrogen, augmented with sufficient diffuse functions to allow accurate representation of the atomic and molecular properties that enter the interaction potential in terms proportional to $[R_{\text{Ne-HF}}]^{-6}$, $[R_{\text{Ne-HF}}]^{-7}$, and $[R_{\text{Ne-HF}}]^{-8}$. The energy was calculated for a range of relative Ne-HF geometries and corrected for basis set superposition effects.[12] The decoupling of the HF vibrational mode justified our holding the HF distance fixed at R_e; in effect we assume the same coupled-electron-pair approximation surface for Ne-FH ($v=1$) and Ne-HF ($v=0$) states. The strongest binding of -65 cm^{-1} was found for the linear NeHF configuration, with a secondary -39-cm^{-1} well in the linear NeHF geometry and an intervening saddle point at -27 cm^{-1}. A variational method in a discrete basis yielded the bound rovibrational eigenstates, and the positions and widths of dissociative (resonance) states were determined from atom-diatom scattering calculations in a rotational close-coupling framework. Infrared transition intensities were calculated assuming the transition dipole to lie along the HF axis.

In addition to the ground vibrational state ($D_0=22$ cm^{-1}), the potential surface supports two bound excited states of the van der Waals (Ne-HF) stretching mode, all of which lie above the barrier to internal HF rotation. The two stretch-excited states have essentially no transition dipole to the ground state, are unlikely to be observable, and do not play a part in what follows. For example, the calculated 16.479 cm^{-1} for $J=0 \rightarrow 1$ transition to the lowest excited Σ stretch state has an intensity 3 orders of magnitude less than that of the fundamental HF excitation. The lowest-lying states in which the HF Σ or Π internal rotational mode (see Fig. 1) is excited were calculated to lie 37.440 and 44.065 cm^{-1} above the ground state, with transition intensities of 30 and 50
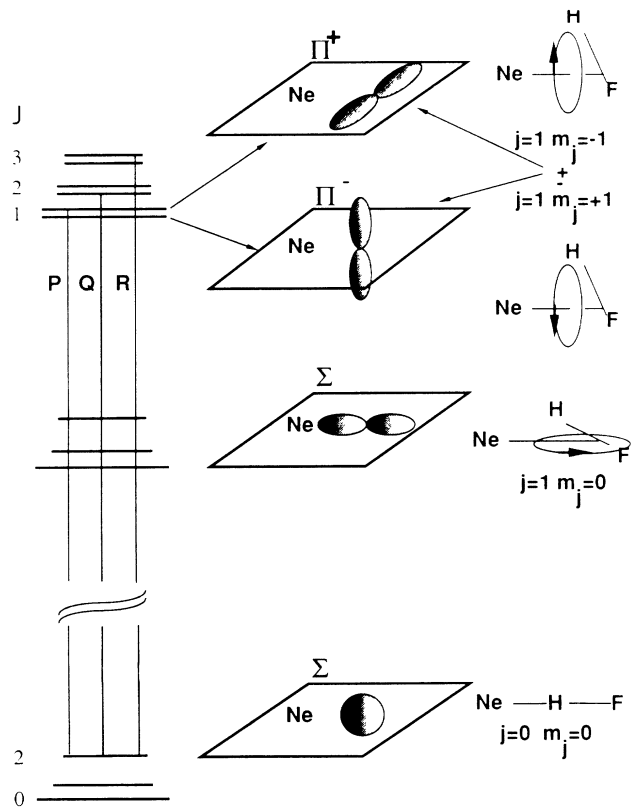
FIG. 1. Partial energy-level diagram for the NeHF van der Waals complex. The rotational stacks of increasing J arise from a sequence of the approximate quantum number l (see text). The states are labeled by the projection of the HF rotor angular momentum j on the figure axis, and are represented by schematic "snapshots" of the HF rotor wave functions with respect to the plane of rotation of the complex. The Π^+ and Π^- rotational states are linear combinations of the $m_j = \pm 1$ states, and have no easily represented classical analog. For nonzero J, Π^+ states (Ref. 9) are mixed with the short-lived Σ states and rotationally predissociate, while the Π^- states are unaffected and remain sharp resonances. The transitions labeled Q and R are present in the spectrum in Fig. 2. Transitions labeled P are observed but not shown in Fig. 2, and transitions to the upper Σ state are too broad to be observable.
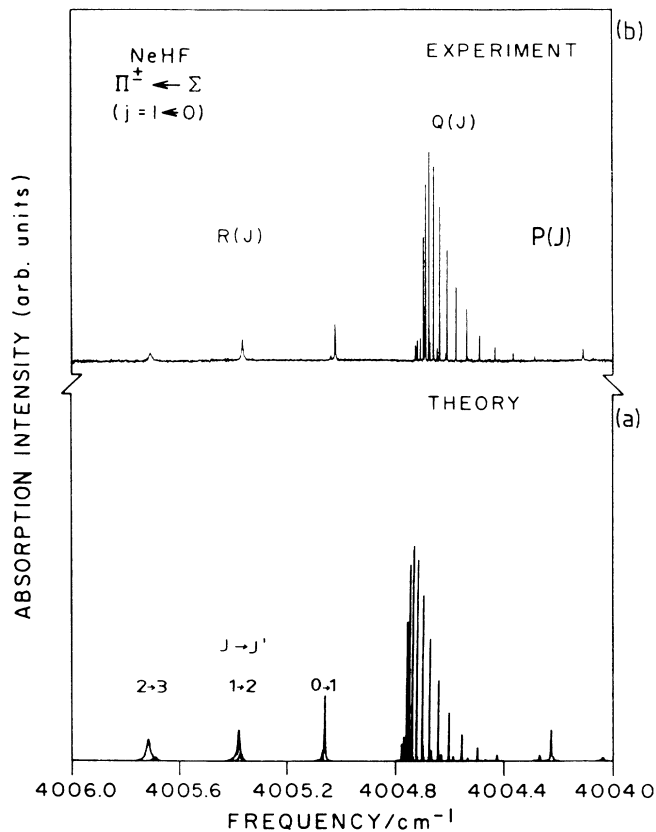

FIG. 2. Infrared spectrum of NeHF: (a) line positions, widths, and intensities derived from *ab initio* electronic structure and nuclear vibrational analysis calculations (Ref. 13); (b) measured with the supersonic slit expansion technique.

times that of the fundamental, respectively. Relative to isolated Ne+HF ($j=0$) these states are metastable by 15 and 22 cm^{-1}, portending vibration-rotation dynamics very different from that in Ar-HCl,[4-7] for example, where the Σ bend and Π bend states are bound.

Excitation of both Π states and the fundamental HF stretch mode were predicted to be sufficiently intense to permit observation by the experimental methods described below, but the calculated linewidth of the Σ bend state is 0.3 cm^{-1}, too broad for reliable detection above the experimental background. The calculated linewidths of the metastable Π^+ state,[9] which can dissociate via J-dependent Coriolis coupling with the short-lived Σ state, were predicted to be narrower, about 0.003 cm^{-1} for

$J=1$, and to increase as $J(J+1)$. In dramatic contrast, the calculated linewidths were negligibly small for the Π^- state, which can dissociate only via vibrational coupling with the HF stretch. The extreme weakness of this coupling means that even though a dissociative channel is energetically open, the Π^- state remains a narrow resonance, essentially a bound state in the continuum. In Fig. 2(a) we present the relevant portion of the infrared spectrum, incorporating the line positions, widths, and relative intensities calculated from first principles.[13]

The spectrum of NeHF was measured with direct absorption infrared laser spectroscopy in a slit supersonic jet. The experimental apparatus and technique have been described in detail elsewhere.[14] Briefly, narrow-band (< 5 MHz) tunable infrared laser light is generated by nonlinear difference frequency mixing,[15] a frequency-stabilized dye laser, and an Ar ion laser in a temperature-phase-matched LiNbO$_3$ crystal. The infrared output is split into two beams, one of which propagates through a twelve-pass White cell surrounding the 4.0-cm-long slit supersonic jet. Both beams are focused onto matched InSb detectors, and the resulting signals subtracted to reduce amplitude fluctuations to levels near

1577

that of the shot noise. NeHF is formed during the adiabatic expansion of a mixture of 1% HF in a 70%/30% mixture of Ne and He. The diminution of the transmitted power is used to probe the transient absorption by complexes passing through the laser beam.

The nozzle and expansion gas are precooled to 250 K to enhance formation of the weakly bound NeHF complex. After subsequent expansion, typical rotational temperatures of 5–7 K are obtained. Transition frequencies are measured with a traveling λ-meter interferometer,[16] and are obtained to a precision and accuracy of 0.0002 cm^{-1} by our referencing to nearby infrared frequency standards.[17] The slit expansion geometry collapses the velocity distribution along the slit dimension, and thus reduces the inhomogeneous Doppler broadening in the spectra by about an order of magnitude. With this intrinsic Doppler narrowing, the resolution of the apparatus is approximately 50 MHz with Ne/He mixtures. This effect enhances detection sensitivity and permits accurate measurement of line broadening due to predissociation in the excited complexes, as discussed below.

A segment of the measured NeHF infrared spectrum in the vicinity of the Π^- and Π^+ origin is shown in Fig. 2(b).[18] Since both this $\Pi \leftarrow \Sigma$ spectrum and the fundamental $\Sigma \leftarrow \Sigma$ spectrum will be discussed in detail elsewhere,[19] we point out here only three noteworthy features. The first is the excellent agreement between the ab initio predictions and the observed line positions. The rotational structure in the spectrum is nearly quantitatively predicted, with the $\Pi^+(J=1)$ combination predicted at 44.065 cm^{-1} above the fundamental HF stretch $(J=0)$ and observed at 44.054 cm^{-1}. One must bear in mind that of the 44-cm^{-1} transition energy, $2B_{HF}$ (approximately 42 cm^{-1}) is due solely to rotational excitation of the HF, and would be accounted for with any completely isotropic surface. However, in the same limit, j and l become rigorously good quantum numbers, the allowed transitions reduce to $\Delta j = \pm 1$, $\Delta l = 0$, and all predissociation linewidths vanish, i.e., behavior qualitatively different from that observed and calculated here. Thus the successful ab initio predictions imply that the anisotropy of the potential surface has been accurately calculated, although characteristics such as the absolute well depth remain untested pending measurements on the deuterated complex.

The second noteworthy feature illustrated in Fig. 2(b) is the strongly red-degraded Q branch, which results from a large negative $\Delta B(\Delta B/B = -1.33\%)$. By comparison with spectroscopic constants obtained from the fundamental HF stretch, approximately half of the decrease in B is due solely to excitation of the bend, in agreement with the red-degraded Q branch predicted theoretically. Third, although internal rotational predissociation and J-dependent linewidths in P and R branch transitions have also been observed in Ar-Hd by McKellar[20] and analyzed by Hutson and LeRoy,[21] we believe the dramatic differences between the linewidths in the P

and R branches, which increase rapidly with J, and the widths in the Q branch, which are broadened only instrumentally, are unprecedented. For a transition into a Π state, the Q branch accesses only the Π^- levels, whereas the P and R branches access the Π^+ levels, and the different linewidth behavior is explained by the different degrees to which the Π^+ and Π^- couple with the dissociative Σ state. As described above, the Σ state itself is too short lived to be observed with any discrete rotational structure. Experimentally observed but not shown in Fig. 2 is the excitation of the fundamental HF stretch, shifted 0.4722 cm^{-1} to the red from the isolated HF line and with an intensity about $\frac{1}{50}$ that of the Π bend.

Our calculations and measurements demonstrate the novel dissociation dynamics of the NeHF van der Waals system, and our measurements constitute the first experimental observation of NeHF. The agreement between the experimental and theoretical spectra suggests that reliable first-principles calculations may now be feasible for weakly bound complexes with as many as twenty electrons.

(a)Permanent address: University Chemical Laboratory, Lensfield Road, Cambridge CBV2 1EW, United Kingdom.
(b)Quantum Physics Division.

[1]C. M. Lovejoy, M. D. Schuder, and D. J. Nesbitt, J. Chem. Phys. 85, 4890 (1986).
[2]G. T. Fraser and A. S. Pine, J. Chem. Phys. 85, 2502 (1986).
[3]C. M. Lovejoy and D. J. Nesbitt, Chem. Phys. Lett. 147, 490 (1988).
[4]B. J. Howard and A. S. Pine, Chem. Phys. Lett. 122, 1 (1985).
[5]C. M. Lovejoy and D. J. Nesbitt, Chem. Phys. Lett. 146, 582 (1988).
[6]D. Ray, R. L. Robinson, D.-H. Gwo, and R. J. Saykally, J. Chem. Phys. 84, 1171 (1986). See also related articles by R. L. Robinson, D.-H. Gwo, D. Ray, and R. J. Saykally, J. Chem. Phys. 86, 5211 (1987); R. L. Robinson, D. Ray, D.-H. Gwo, and R. J. Saykally, J. Chem. Phys. 87, 5149 (1987); R. L. Robinson, D.-H. Gwo, and R. J. Saykally, J. Chem. Phys. 87, 5156 (1987); K. L. Busarow, G. A. Blake, K. B. Laughlin, R. C. Cohen, Y. T. Lee, and R. J. Saykally, Chem. Phys. Lett. 141, 289 (1987).
[7]M. D. Marshall, A. Charo, H. O. Leung, and W. Klemperer, J. Chem. Phys. 83, 4924 (1985).

[8]For earlier *ab initio* calculations of the NeHF potential-energy surface see M. Losonczy, J. W. Moskowitz, and F. H. Stillinger, J. Chem. Phys. **61**, 2438 (1974); P. W. Fowler and A. D. Buckingham, Mol. Phys. **50**, 1349 (1983); A. J. Stone and I. C. Hayes, Faraday Discuss. Chem. Soc. **73**, 19 (1984); G. A. Gallup and J. Gerratt, J. Chem. Phys. **83**, 2316 (1985). While all the earlier calculations predicted a linear NeHF structure, we believe that the current calculations go substantially further in accounting for the electron correlation important in dispersion energy and for long-range induction effects. This explains, in part, the differences between the current and the earlier results.

[9]The historical notation is potentially confusing. The post superscript of the Π^+ and Π^- state labels refers to the symmetry of these states under reflection in a given plane, in the current context the plane in which the Ne and HF centers of mass rotate.

[10]S. V. ONeil, D. C. Clary, D. J. Nesbitt, H.-J. Werner, and P. Rosmus, "Weakly Bound NeHF" (to be published).

[11]The coupled-electron-pair approximation wave function includes single and double electron excitations from a single determinant reference state, and approximates contributions from quadruple replacements. See W. Meyer, J. Chem. Phys. **58**, 1017 (1973).

[12]Basis set superposition effects were corrected with the functional counterpoise method of S. F. Boys and F. Bernardi, Mol. Phys. **19**, 553 (1970).

[13]The calculated infrared spectrum is derived by adding the Ne-HF $(v=1 \leftarrow 0)$ transition energy to the rovibrational eigenvalues of the *ab initio* potential surface.

[14]C. M. Lovejoy and D. J. Nesbitt, J. Chem. Phys. **86**, 3151 (1987).

[15]A. S. Pine, J. Opt. Soc. Am. **64**, 1683 (1974).

[16]J. L. Hall and S. A. Lee, Appl. Phys. Lett. **29**, 367 (1976).

[17]G. Guelachvili, Opt. Commun. **19**, 150 (1976).

[18]The small peaks to the blue of each Q and R branch line are due to HF complexed with ^{22}Ne, which has a 10% natural abundance.

[19]C. M. Lovejoy, D. C. Clary, and D. J. Nesbitt, to be published.

[20]A. R. W. McKellar, Faraday Discuss. Chem. Soc. **73**, 89 (1982).

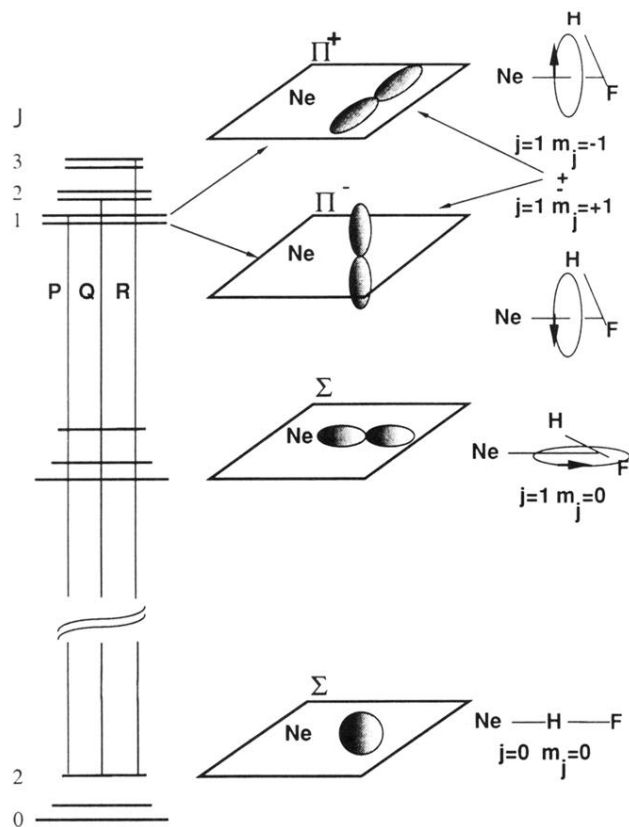[21]J. M. Hutson and R. J. LeRoy, J. Chem. Phys. **78**, 4040 (1983).

FIG. 1. Partial energy-level diagram for the NeHF van der
Waals complex. The rotational stacks of increasing J arise
from a sequence of the approximate quantum number l (see
text). The states are labeled by the projection of the HF rotor
angular momentum j on the figure axis, and are represented by
schematic "snapshots" of the HF rotor wave functions with
respect to the plane of rotation of the complex. The Π^+ and
Π^- rotational states are linear combinations of the $m_j = \pm 1$
states, and have no easily represented classical analog. For
nonzero J, Π^+ states (Ref. 9) are mixed with the short-lived Σ
states and rotationally predissociate, while the Π^- states are
unaffected and remain sharp resonances. The transitions la-
beled Q and R are present in the spectrum in Fig. 2. Transi-
tions labeled P are observed but not shown in Fig. 2, and tran-
sitions to the upper Σ state are too broad to be observable.